Iran J Pharm Res. 2022 December; 21(1):e126912. doi: 10.5812/ijpr-126912.
Published online 2022 May 8. **Research Article**

# The Preparation, Biodistribution, and Dosimetry of Encapsulated Radio-Scandium in a Dendrimer for Radio-nano-pharmaceutical Application

Leila Moghaddam-Banaem [1,*], Navideh Aghaei Amirkhizi [2], Sodeh Sadjadi [2], Fariba Johari-Deha [2] and Mitra Athari-Allaf [3]

[1] Nuclear Fuel Cycle School, Nuclear Sciences and Technology Research Institute (NSTRI), Tehran, Iran
[2] Radiation Application School, Nuclear Sciences and Technology Research Institute (NSTRI), Tehran, Iran
[3] Department of Medical Radiation Engineering, Sciences and Research Branch, Islamic Azad University, Tehran, Iran

[*] *Corresponding author*: Nuclear Fuel Cycle School, Nuclear Sciences and Technology Research Institute (NSTRI), Tehran, Iran. Email: lmoghaddam@aut.ac.ir

**Received** 2021 October 13; **Revised** 2022 January 09; **Accepted** 2022 January 23.

**Abstract**

This study aimed to investigate the synthesis, characterization, and biodistribution of scandium nanoparticles encapsulated within poly (amidoamine) (PAMAM) dendrimers, as well as to estimate the human absorbed dose. It also aimed to examine, in particular, the amine-terminated PAMAM dendrimers in generation 5. Irradiation of the compound in the nuclear reactor resulted in the formation of Sc-radioactive complex nanoparticles. The compound of the dendrimer-$Sc^{3+}$ was confirmed by the UV-vis spectrometer. The size of the particles was less than 10 nm, and it was assessed using high-resolution transmission electron microscopy (HRTEM) and dynamic light scattering (DLS). The synthesized complex was irradiated by the $3 \times 10^{11}$ $n.cm^{-2}s^{-1}$ flux of neutron for 2 h. Mice bearing a breast tumor were employed to assess the therapeutic dose that was delivered by the poly scandium-46-nanoparticles. As opposed to the untreated groups, a single injection of poly phosphate-buffered saline to intratumoral in other groups to deliver a dose of 100 $\mu$Ci resulted in a statistically significant 39.24% reduction in tumor volume 14 days after injection. After applying the biokinetics data in mice, the human's absorbed dose from scandium-47 encapsulated PAMAM was extrapolated based on animal data. The absorbed doses in critical organs, including the liver, lung, spleen, kidney, and bone, were 0.879, 0.0472, 0.191, 0.107, and 0.155 mGy/MBq, respectively.

*Keywords:* PAMAM G5, Radio-scandium, Encapsulation, Solid Tumor, Dosimetry

## 1. Background

The radiation therapy is mostly aimed at delivering a lethal dose of radiation to the tumor while sparing the surrounding normal tissue unharmed (1-4). This approach leads to the development of radiopharmaceuticals. The application type of a radiopharmaceutical is depended on the carrier's characteristics and the radionuclide that is incorporated in tracer amounts. The chemical structure of carrier may be an organic or inorganic molecule, an antibody, a peptide, or a more complex structure, such as nanoparticles with the ability to concentrate in a pathological site. The therapeutic or diagnostic utilization of the radiopharmaceutical is determined based on the radionuclide type of the decay that joins to the carrier. The fundamental aim of radiopharmaceutical is to accumulate in the tumor area in order to deliver the required dose, without exposing the normal tissues to unnecessary harmful radiation (5-8).

Dendrimers are specified as synthetic polymers with a three-dimensional shape, highly branched architecture, monodispersity, and nanometric size range (9, 10). The structure of dendrimer consists of three areas: a core, several branches, and diverse surface groups (11). DENs have been the focus of research attention recently because they have the desired chemical and physical properties of the encapsulated nanoparticles along with the adjustable solubility and surface reactivity. Furthermore, the dendrimer structure, as well as the process of introducing the metal ions into the dendrimer can control other characteristics of the nanoparticle, such as size, composition, and structure. DENs have several potential applications; however, this study aimed to explore the therapy application (12-15).

Considerable research attention has been recently given to poly (amidoamine) (PAMAM) dendrimers in radioimmunotherapy as targeted drug carriers, delivery agents, and imaging agents in human systems for cancer therapy. The structure of PAMAM dendrimers consists of alkyldiamine core and tertiary amine branches. They are provided in 10 generations that differ in core types and functional surface groups. The increase in the number of generations leads to increase in molecular diameters, doubling of the number of reactive surface sites, and increase in the molecular weight of the preceding generation. Studies investigating the labeling of 10 generations of PAMAM; G3, G4, and G5 have demonstrated that the proper medical applications' characteristics and G5 PAMAM dendrimer have potential to control the properties of therapeutic moieties and to cause low toxicity (2, 10, 13, 14, 16, 17).

Application of radionuclide for labelling PAMAM including $^{99m}$Tc and $^{111}$In for SPECT imaging as well as $^{68}$Ga, and $^{64}$Cu for PET imaging, has generated satisfactory results. Recently, $^{177}$Lu has given priority to the development of therapeutic dendrimers when applying radionuclide therapy. The 12 radionuclides with $\beta^-$ emition that have been used in preclinical and clinical research for labeling the dendrimers are shown in Table 1 (18). The application of radiotherapeutic $\beta^-$ emitters with a low ratio of gamma photons ($\gamma$) in the suitable range (80 to 200 keV) is also desirable for nuclear imaging. These radionuclides with theranostic properties are valuable for the nanometric clinical radiotherapeutic applications. Well-established coordination chemistry of dendrimers boosts the development of new series of the labelled dendrimers by radiometals (19).

Scandium is a metallic element with silvery-white color, extracted from various rare minerals, and is also a by-product of uranium ores processing. The only naturally occurring isotope is scandium-45. Among the scandium radionuclides, the scandium-44 and scandium-47 have attracted more attention due to their diagnostic and therapeutic applications (20).

Scandium-47 is a low-energy beta emitter with 3.35 d half-life and 162 keV average $\beta^-$ energy, suitable for tumor therapy. These nuclear specifications are similar to Lutetium-177 ($T_{1/2}$ = 6.65 d; $E_{\beta av}$ = 134 keV; E$\gamma$ = 113, 208 keV) that are well-established clinically. Comparing the nuclear characteristics and the average tissue ranging between $^{47}$Sc and Lutetium-177 has revealed that the average tissue range of $^{47}$Sc (0.2 mm) longer than $^{177}$Lu (0.16) and the half-life of $^{177}$Lu (6.7 d) longer than $^{47}$Sc (3.35 d) make $^{47}$Sc a suitable agent for radioimmunotherapy. Since the red marrow absorbed dose imposes a limitation on the targeted radionuclide-therapy, the lower half-life of scandium-47 compared to that of Lutetium-177 is regarded as an advantage for this radionuclide (21).

Recent studies have documented the successful combination of scandium-47 with small-molecular-weight and peptide-based agents for conjugation with fast blood clearance. Scandium-47 has also been proposed to employ for performing radioimmunotherapy (22-26).

Taking into account the scarcity and high cost of scandium-47 isotope, initial investigations in our study were conducted using scandium-46, which was chemically equivalent. The half-life of scandium-46 is 83.8 days, and also has a high-energy beta-emissions. These nuclear properties make scandium-46 an ideal alternative for analyzing the chemistry, stability, and biodistribution results of the compounds labeled as radio-scandium. These results confirm the feasibility of using scandium-47 for carrying out future experiments. Scandium-46 has been used in many biological studies in the field. Baer et al. (27), for instance, investigated the labeling microsphere using scandium-46 radionuclide in order to measure the increment of the myocardial blood flow. Wehner et al. also used scandium-46 to analyze the lungs as a radiotracer (28). Mutsuo and Kazuhisa (29), on the other hand, investigated the potential cosmogenic application of scandium-46 in order to explore the evolutionary process of chondrites after isolating from the parent body. Scandium-46 labeled microsphere has also been used vastly for determining the blood flow in many cardiovascular studies (30).

The present study aimed to develop a procedure for preparing the encapsulated natural scandium nanoparticles and irradiating them in Tehran Research Reactor (TRR) in order to produce dendrimer and encapsulate scandium-46 nanoparticles. Scandium-46 can be produced by exercising thermal neutron irradiation of natural scandium target with 10.4 barn cross-section through $^{45}$Sc (n,$\gamma$)$^{46}$Sc reaction. The PAMAM G5-$NH_2$ dendrimer proved a suitable agent due to creating the ionic bond with scandium-46 as a metal ion in the core and easy location.

## 2. Objectives

This study also aimed to evaluate the biodistribution of the nano-radio-complex in tumoral and safe mice, as well as to estimate the human's absorbed dose from scandium-47 labelled nanoparticles by extrapolating the animals' biodistribution data. It is noteworthy that this estimation

**Table 1.** The Reported Radionuclide for Labelling PAMAM Dendrimer

| Radionuclide | Half-life | Decay Mode | Energy Max (keV) | Max Range in Tissue (mm) |
|---|---|---|---|---|
| **Yttrium-90** | 64.1 h | $\beta$ | 2280 | 12 |
| **Iodine-131** | 8.04 d | $\beta$,$\gamma$ | 807 | 2.4 |
| **Lutetium-177** | 9.5 d | $\beta$,$\gamma$ | 500 | 1.6 |
| **Samarium-153** | 1.95 h | $\beta$,$\gamma$ | 233 | 3 |
| **Strontium-89** | 50.53 d | $\beta$ | 1463 | < 3 |
| **Holmium-166** | 26.9 h | $\beta$,$\gamma$ | 1853 | 10.2 |
| **Rhenium-186** | 3.33 d | $\beta$,$\gamma$ | 1069 | 5 |
| **Rhenium-188** | 17 h | $\beta$,$\gamma$ | 2120 | 11 |
| **Copper-67** | 2.58 d | $\beta$,$\gamma$ | 577 | 2.2 |
| **Promethium-149** | 2.21 d | $\beta$,$\gamma$ | 1070 | 5 |
| **Gold-198** | 2.69 d | $\beta$,$\gamma$ | 1372.8 | 4.4 |

was performed by using MIRDOSE schema and Matlab software.

## 3. Methods

PAMAM-G5-$NH_2$ dendrimer 5wt% in $HNO_3$ and methanol solution, Sodium borohydride ($NaBH_4$), $HClO_4$ (70.0%), and scandium (III) nitrate (Sc $(NO_3)_3$) were obtained from Sigma Aldrich Chemical, Germany. To dilute the scandium salt, the fresh deionized water was used.

Varian Cary3 (USA), spectrometer, and Philips-CN 30 (Netherlands) transmission electron microscope were applied for capturing UV-Vis and high-resolution transmission electron micrographs (HRTEM) with a resolution of 0.23 nm point-to-point. To prepare the samples for capturing HRTEM, a drop of compound was placed on a TEM grid with holey-carbon-coated Cu, due to which the solvent evaporated in the air. EM 3200 KYKY digital scanning electron microscope, China, with a resolution of 6.00nm, was employed to perform the scanning electron microscopy (SEM) test. In order to perform dynamic light scattering (DLS) test, a Zetaplus instrument from Brookhaven Instruments was used to obtain size distribution data. Gamma spectrometry test was performed by using a liquid scintillation type spectrometer from the Wallac 1220 Quantulus, USA. Bertold beta counter (Lb123 Model, Germany) was used as a beta counter. Biodistribution studies with animals were performed according to the guidelines proposed by the United Kingdom's biological council for the application of live animals in the biological scientific investigations.

Female balb/c mice aged 6 - 8 weeks (n = 20, 18 $\pm$ 3 g) and 4T1 cell flask were obtained from Pasteur Institute of Iran. The 4T1 cells were processed by cell culture and cell passage method and then injected into the mice; the solid tumors of breast were developed 10 - 14 days after the injection.

### 3.1. Synthesize of PAMAM Encapsulated Scandium

A 20mM Sc $(NO_3)_3$ solution was prepared from Sc $(NO_3)_3$ and an aqueous solution of 0.01 mM dendrimer with an average of 55 ions of $Sc^{3+}$ per PAMAM (PAMAM-G5-$NH_2$ $(Sc^{3+})_{55}$) was obtained from 0.05 mM PAMAM-G5-$NH_2$ and 20 mM Sc $(NO_3)_3$ (31). The pH was set to 7.5 by 2M NaOH before reduction, and the nitrogen gas flow was used continuously for 20 min to purge the PAMAM-G5-$NH_2$ $(Sc^{3+})_{55}$. The dendrimer-encapsulated $Sc^{3+}$ was reduced to the zero-valent metal G5-$NH_2$ $(Sc)_{55}$ by adding a 3- $NaBH_4$ with a fold molar to the solution, and the reaction was allowed to proceed for 2h under nitrogen atmosphere. The pH of the final solution was set to 3 by $HClO_4$ to decompose the extra amount of $BH^-_4$.

### 3.2. Preparation of PAMAM-G5 Dendrimer Encapsulated Radio-Scandium

The synthesized PAMAM encapsulated scandium was irradiated by neutron flux at the pile position in Tehran Research Reactor (TRR) where neutron fluxes were $3 \times 10^{11}$ $n.cm^{-2}$ $s^{-1}$. The amount of encapsulated scandium in 60mg of the PAMAM encapsulated scandium was 10mg. A quartz ampoule was used to seal the target and, then was adjusted in an aluminium can. Neutron irradiation was performed for 2 hours. After the bombardment and prior to performing the quality control test, the target was allowed to decay

for at least 6 h in order to reduce the short-lived radionuclides' activity in the aluminium holder.

All radioactivity counting identified with paper chromatography was completed utilizing a NaI (Tl) scintillation counter at 396 keV baseline. The HPGe detector and Bertold beta counter (Lb123 Model), Germany were used to assess the activity and radionuclidic purity of the scandium-46 by performing gamma spectroscopy and beta spectroscopy.

### 3.3. Quality Control Techniques

For assessing the radiochemical purity and evaluating the efficiency, the radioactivity of the PAMAM-G5 dendrimer encapsulated radio-scandium was measured after irradiation in the research reactor by adopting instant thin-layer chromatography (ITLC) method and using Whatman no-1 strips. To discriminate free scandium from the radiolabel compound, a solution of 0.1 mM DTPA (diethylene-triamine-penta-acetic acid) was employed as a mobile phase.

The SEM images were obtained in order for evaluating the size and shape of the encapsulated scandium-46 radionanoparticles after irradiation.

### 3.4. The Assessment of In Vitro Stability of Radio-scandium-PAMAM Complex

To investigate the in vitro stability of radio-scandium-PAMAM, the compound was stored in human serum at 37°C and room temperature until 72 hours before conducting the analysis.

Radio-scandium-PAMAM (3.2 MBq (100 $\mu$L)) was added to 900$\mu$L of freshly-prepared human serum and incubated 1 hour at 37°C. Then, 100 microliter aliquots were treated with 100 $\mu$L of ethanol at various times (1, 4, 6, 12, 24, and 48 and 72 hours after reaction). The samples were centrifuged at 3000 rpm for 10 minutes in order to precipitate the serum proteins. Then the supernatants chromatography was performed.

### 3.5. Biodistribution Studies

Biodistribution studies were performed in a reserved area outside the radiopharmaceutical preparation lab. The guidelines regarding the animal experiments issued by national and international agencies were followed in this study.

The experiments were performed in mice weighing 18 - 25g in solid tumoral and normal conditions. The set of animals used in each experiment was of the female sex, strain, and flock of about the same weight.

The biodistribution studies were performed to investigate 3 groups of mouse. In the first group (group A) that included mice bearing solid tumor, the PAMAM-G5 dendrimer encapsulated radio-scandium was injected directly to the tumor site, whereas the second group (group B) was injected in the vein through the tail. No injection was administered to the last group (group C) since it was a control group of tumoral mice. The study was performed 7-10 days after the tumor implantation so as to gain the diameter of tumor mass around 1cm.

In group A, 0.2 mL PAMAM-G5 dendrimer encapsulated radio-scandium solution with 7.4MBq activity was injected directly into the center of the tumor site of the tumor-bearing mice (n = 5). They were sacrificed 2 weeks after the injection, and their organ samples, including liver, lungs, spleen, kidneys, stomach, intestine, femur, bladder, heart, blood, and thyroid gland were removed and placed in containers for measuring their weight and counting. The obtained data were expressed based on %ID/g (percentage of injected dose per gram) to estimate the leakage of radiocompound from tumor tissue to other organs.

In group B, the mice were injected with 0.1 mL of solution with 3.7 MBq activity intravenously and then were sacrificed at the specified time intervals (4, 24, 48, 72h) after the injection. In a similar fashion to group A, the organs from mice in group B were assessed for the absorbed activity as %ID/g. The volume of tumors was estimated by adjusting caliper in two dimensions, and the volume was measured as, where L = length (mm) and W = breadth (mm).

### 3.6. Dosimetry

The mass correction (kg/g) method was adopted for estimating human absorbed dose (32). In the mass correction method, the biodistribution data of animal are applied to human data (33) in the form of a percentage of the injected dose. The mass data of 73kg standard adult male were obtained from ICRP89 (34).

The residence time ($\tau$) (Bq-h/Bq) calculation and the cumulated activities in source organs were expressed based on the %ID versus the time for each organ that had been described in our previous article (24).

Finally, the calculation of the absorbed doses of human organs was performed according to the MIRD technique (35), by applying MIRDOSE software with the S-values

of scandium-47and the estimated residences time. The source organs for MIRDOSE software were considered as follows: liver, bone, kidney, spleen, red marrow, pancreas, muscle, thyroid, and remainder of the organs. The accumulated activity in the bone was presumed equally divided between trabecular and cortical bone.

## 4. Results

### 4.1. Characterization of PAMAM-G5 Dendrimer Encapsulated Radio-Scandium

Figure 1A shows the UV-Vis spectra of Sc $(NO_3)_3$ and PAMAM-G5-$NH_2$ $(Sc^{3+})_{55}$. The appearance of an absorption band with $\lambda$ max of 300 nm confirmed the formation of dendrimer-$Sc^{3+}$ complex (this band arises from a ligand to metal charge-transfer (LMCT) transition). In addition, the absorption band at 270 nm associated with Sc $(NO_3)_3$ was disappeared, indicating the absence of free scandium ions.

Figures 1B and C show the size and size distribution of prepared nanoparticles that were determined using HRTEM and DLS analyses (Table 2).

### 4.2. Production and Quality Control of Nano-radiopharmaceutical

The radiochemical purity, size, and shape of PAMAM-G5 dendrimer encapsulated radio-scandium after irradiation in the research reactor were measured by adopting instant thin-layer chromatography (TLC) and SEM. The specific activities were 0.2 mCi/mg and 13.08 mCi/mg for scandium and Sc-PAMAM [47], respectively.

The SEM of PAMAM-G5 dendrimer encapsulated radio-scandium after synthesis proved the spherical and nano size of the complex; after irradiation in the reactor by thermal neutron flux, however, the volume was increased by more than 10-fold before the irradiation. This effect is shown in Figure 2A and B.

In the chromatographic system where DTPA was employed as a mobile phase, the $^{46}Sc$ $(NO_3)_3$ moved towards the solvent front; while the PAMAM-G5 dendrimer encapsulated radio-scandium stayed at the place of spotting. The radiochemical purity of the complex was found to be higher than 95% at room temperature (Figure 3A and B). The $R_f$ value was 0.7 for $Sc^{3+}$ ion, and it was 0.2 for the complex.

The results of the in vitro stability test (Figure 4) demonstrated approximately %92 stability at room temperature, and %90 in human serum during 48h after complexation. The results showed that the radio-scandium-PAMAM was stable until 48h, which was comparable with its half-life; hence, the radio-scandium-PAMAM was confirmed to be stable in terms of efficiency.

### 4.3. Biodistribution Studies

Figure 5 shows the biodistribution of the PAMAM-G5 dendrimer encapsulated radio-scandium in group A at specified times that were obtained from counting of the organs and, as it can be seen, the leakage of the complex to the other organs was approximately negligible. The tumor sizes in mice of group A are shown in Figure 6. The sizes of tumors were calculated before injection and 14days after direct intra-tumoral injection. The untreated control groups are presented in the last columns of the diagram. These results suggested that the volume of tumors was decreased by up to 39.24%. Figure 7 shows the biodistribution of the PAMAM-G5 dendrimer encapsulated radio-scandium in group (B) after intravenous injection at specified times.

### 4.4. Dosimetry

The calculated %ID (percentage of injected activity) for humans based on the extrapolation of %ID/g data of mice is shown in Figure 8. After applying the estimated %ID (percentage of injected activity) to human, the residence times and cumulated activities of source organs were calculated by using non-linear regression analysis and MATLAB software (Table 3) (32).

After estimation of the residence times, they were used to get the absorbed doses of organs by adopting MIRDOSE schema, and the results are represented in Table 4. As shown in Table 4, the absorbed doses in sensitive organs like the liver, lung, spleen, bone, and kidney were 0.879, 0.0472, 0.191, 0.155, and 0.107 mGy/MBq, respectively.

## 5. Discussion

The present study mostly aimed to differentially estimate the preparation of metal PAMAM-G5 dendrimer encapsulated scandium. This was primarily achieved by the complexation of metal ions with interior amine groups of the dendrimer and, then, chemical reduction, which resulted in the corresponding PAMAM-G5 dendrimer encapsulated scandium nano-particles. The results of UV-Vis spectra as well as HRTEM and DLS confirmed that the dendrimer-assisted protocol had the potential to provide well size-controlled scandium nanoparticles with narrow

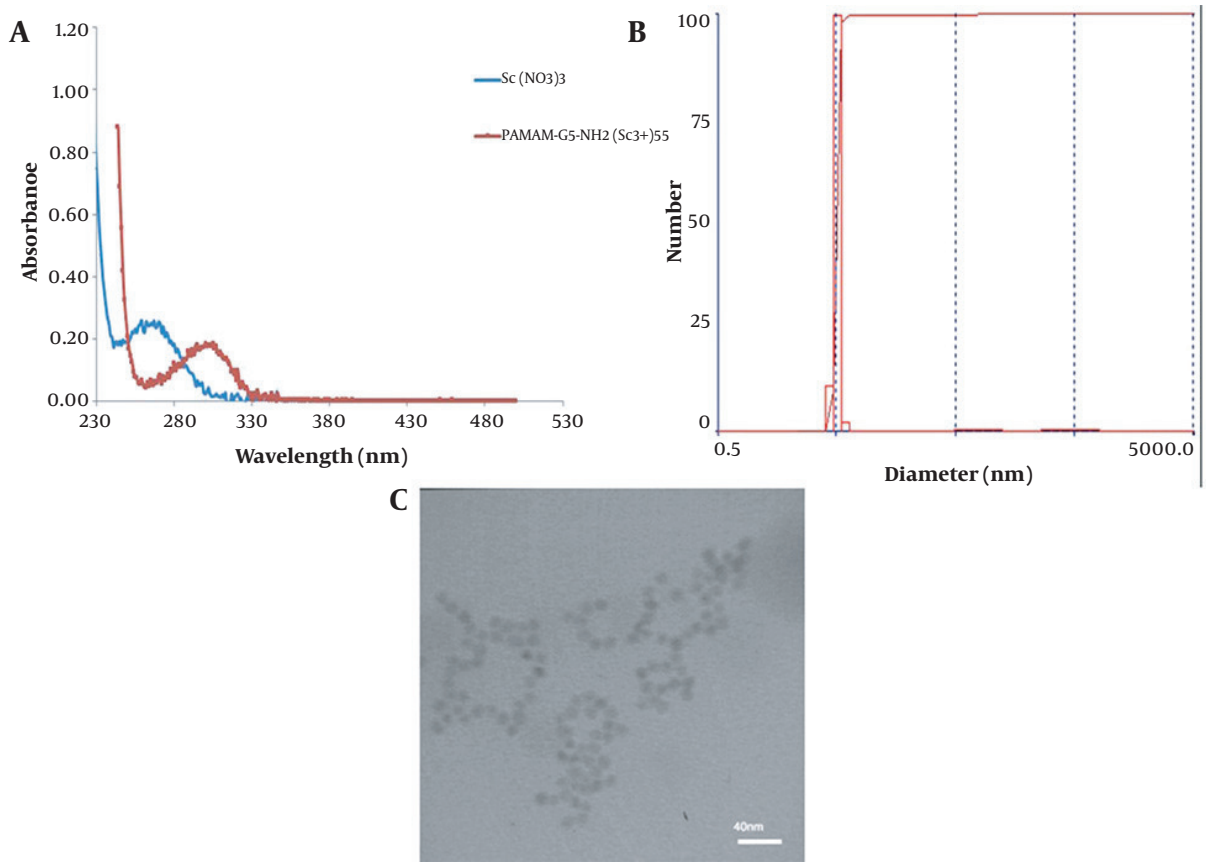


**Figure 1.** A, UV-Vis absorbance spectrum of solution containing 0.55 mMSc $(NO_3)_3$, G5-$NH_2$ $(Sc^{3+})_{55}$; B, dynamic light scattering (DLS) results of G5-$NH_2$ $(Sc^{3+})_{55}$; and C, the result of high resolution transmission electron microscopy (HRTEM)

**Table 2.** Study of Dynamic Light Scattering

| d (nm) | G (d) | C (d) | d (nm) | G (D) | C (D) | d (nm) | G (D) | C (D) |
|---|---|---|---|---|---|---|---|---|
| 2.6 | 0 | 0 | 20.5 | 0 | 96 | 161.4 | 0 | 100 |
| 3.1 | 0 | 0 | 24.7 | 0 | 96 | 194.7 | 0 | 100 |
| 3.7 | 0 | 0 | 29.8 | 0 | 96 | 234.9 | 0 | 100 |
| 4.3 | 7 | 6 | 35.9 | 0 | 96 | 283.4 | 0 | 100 |
| 5.1 | 100 | 93 | 43.4 | 0 | 96 | 341.9 | 0 | 100 |
| 5.9 | 3 | 96 | 52.3 | 0 | 96 | 412.5 | 0 | 100 |
| 6.9 | 0 | 96 | 63.1 | 2 | 98 | 497.7 | 0 | 100 |
| 8.1 | 0 | 96 | 76.2 | 2 | 100 | 600.5 | 0 | 100 |
| 11.7 | 0 | 96 | 91.9 | 0 | 100 | 724.5 | 0 | 100 |
| 14.1 | 0 | 96 | 110.9 | 0 | 100 | 874.1 | 0 | 100 |
| 17.0 | 0 | 96 | 133.8 | 0 | 100 | 1054.5 | 0 | 100 |

Abbreviations: d, nanoparticles diameter (nm); G, gussian nanoparticle diameters; C, cumulative nanoparticles diameter.

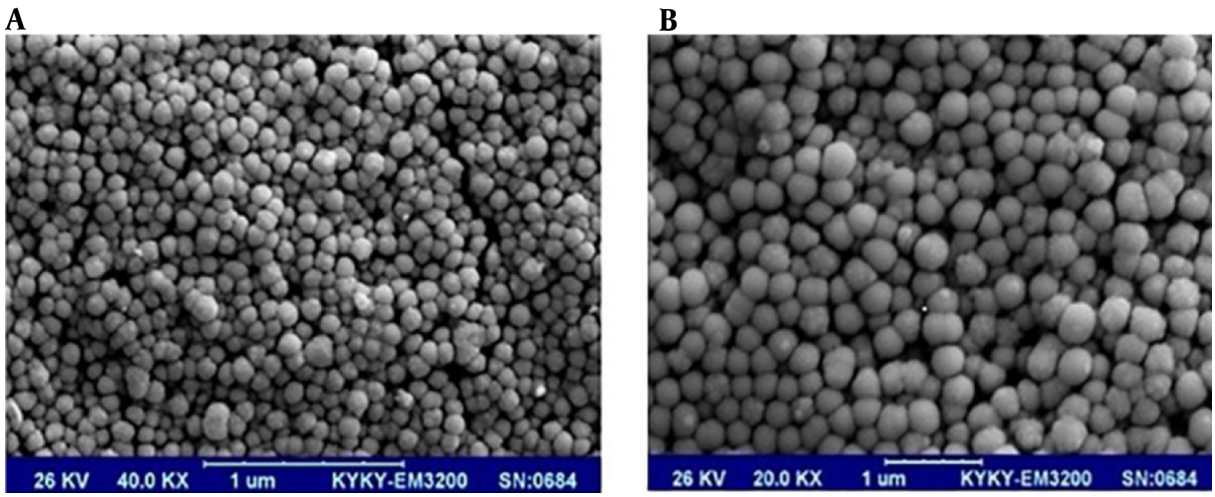


**Figure 2.** Scanning electron microscopy (SEM) of scandium-PAMAM nanoparticles; A, before neutron irradiation; B, after neutron irradiation

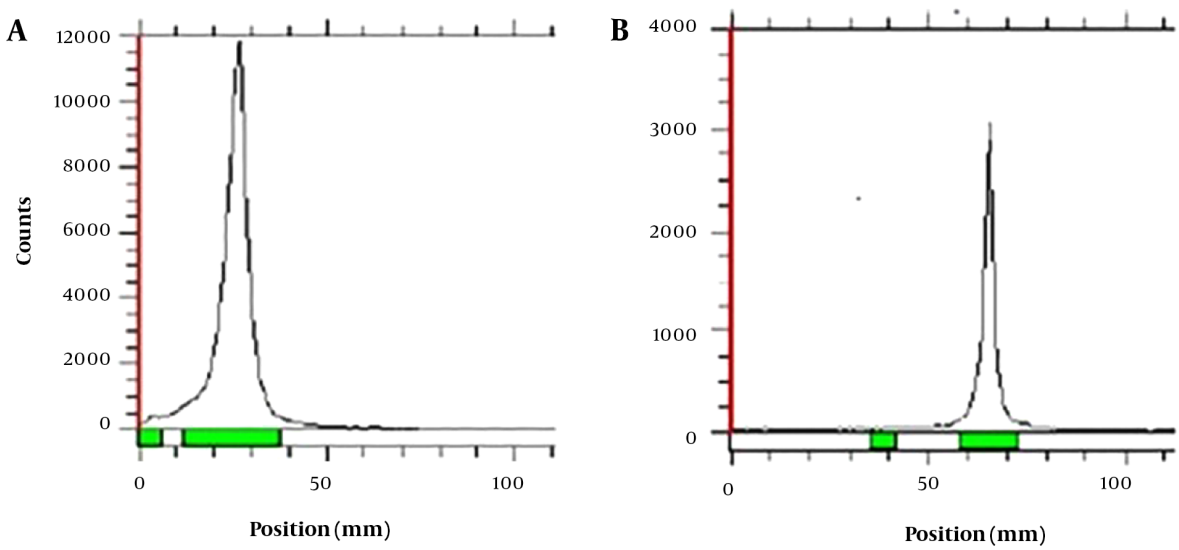


**Figure 3.** Paper radio chromatogram of: A, PAMAM-G5 dendrimer encapsulated radio-scandium and; B, Sc $(NO_3)_3$ eluted by DTPA 0.1 mM/L

size distribution (5 - 10 nm). The synthesized nanoparticles showed a spherical shape with an average size of 5 nm; however, no particle agglomeration was detected. After irradiation of the PAMAM-G5 dendrimer encapsulated scandium in the reactor by the flux of thermal neutron, the results of SEM showed polymerization of the nanoparticles, but the spherical shapes of nanoparticles were reserved.

The biodistribution of the complex in the group of mice who received a direct injection in the center of their tumors showed that the leakage of the complex to the other organs was approximately negligible. The tumor size in this group was decreased by up to 39.24% in comparison to that in untreated control group. The vein injection was performed for precise evaluation of the biodistribution of the complex in the organs. The biodistribution of the PAMAM-G5 dendrimer encapsulated radio-scandium revealed that the maximum uptakes were in the lung, spleen, and, liver, which represented the distribution model of nanoparticle. This biodistribution was in accordance with the biodistribution of nanoparticles due to the

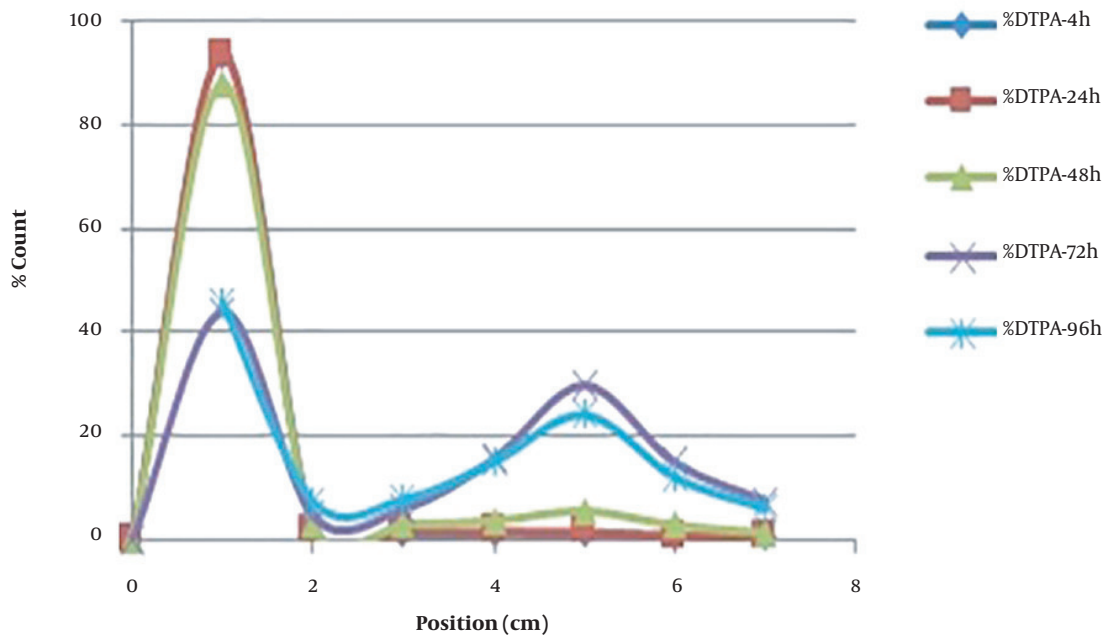


**Figure 4.** The in vitro test by ITLC with Dtpa 0.1 mM/L as mobile phase

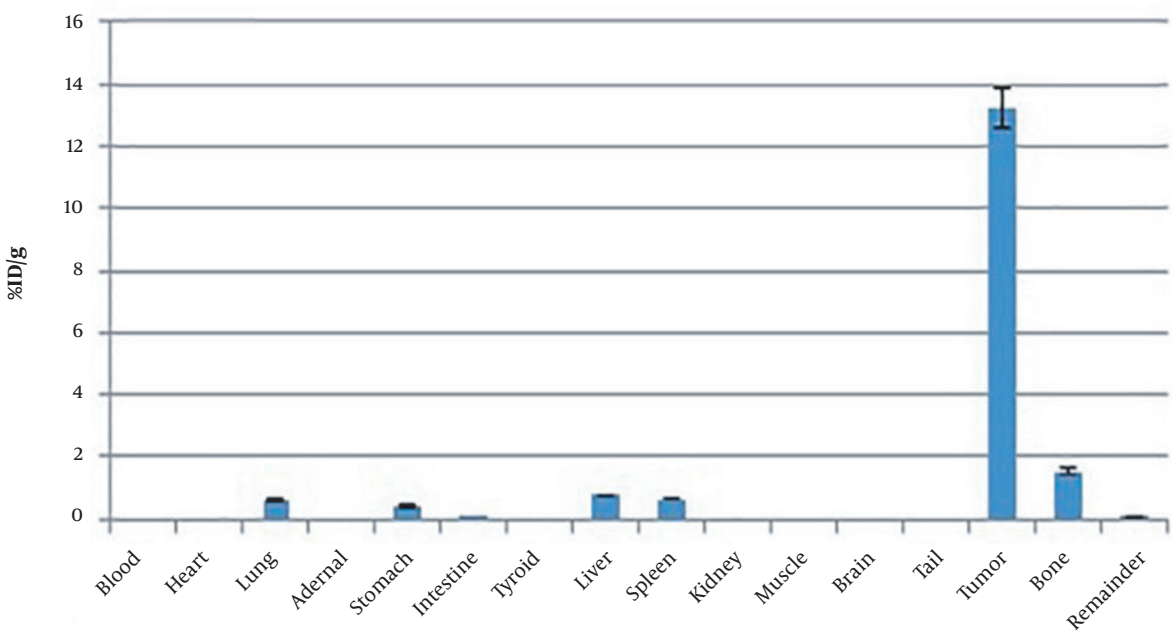


**Figure 5.** The biodistribution of the radio-compound in group A that the nano-radio-scandium-PAMAM was injected directly to the center of the tumor.

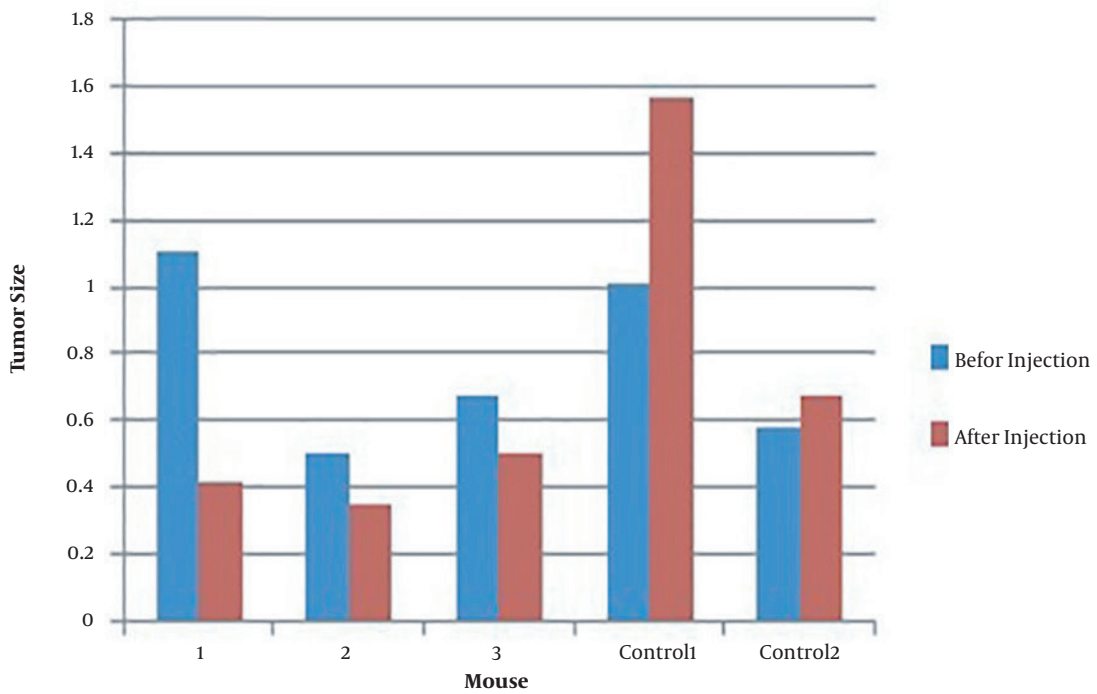


**Figure 6.** Tumors' size before and after intra-tumoral injection. Control 1 and control 2 were mice group without injection.

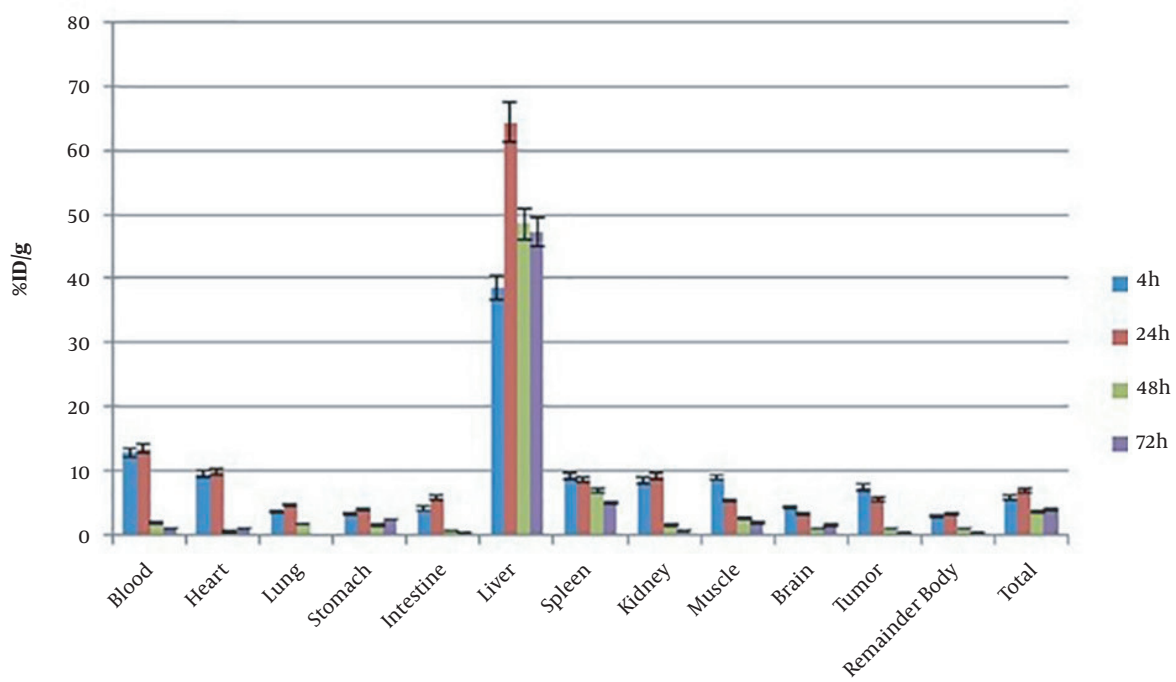


**Figure 7.** %ID/g data for group A that the nano-radio-scandium-PAMAM was injected intravenously through the tail vein of mice; 4, 24, 48, and 72 hours later.

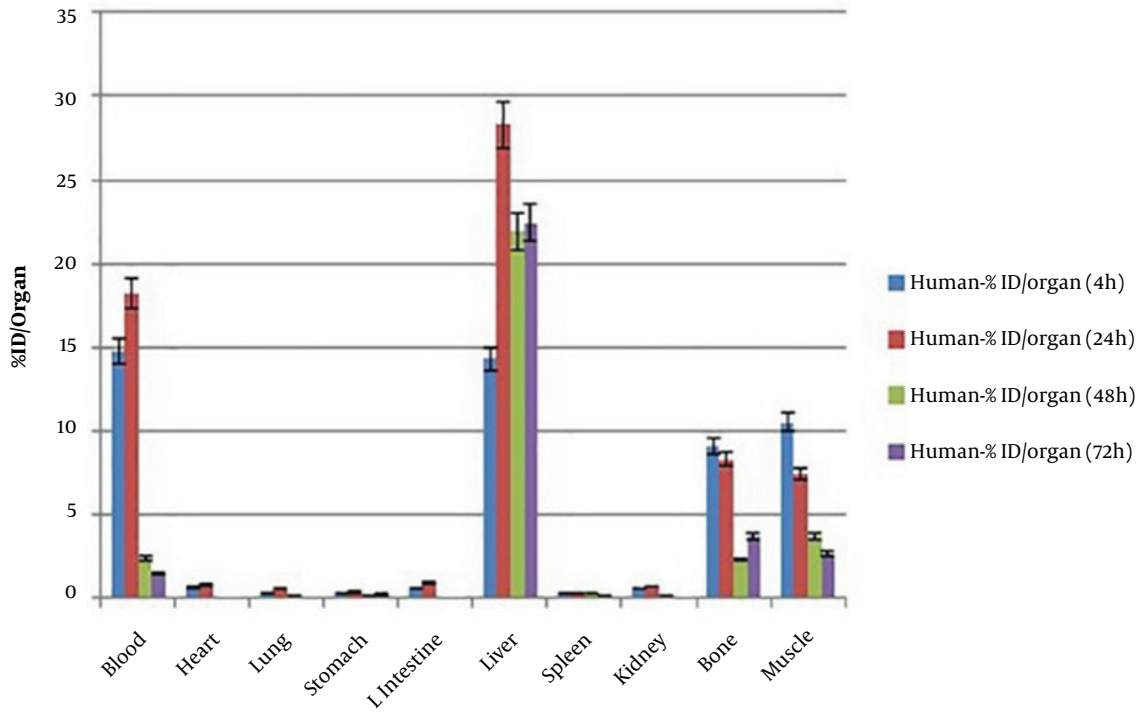


**Figure 8.** %ID/organ of human that was extrapolated from mice %ID/g

**Table 3.** The Estimated Source Organs' Residence Times of the Human

| Residence Times | Hour |
|---|---|
| **LLI** | 0.31 |
| **Stomach** | 0.17 |
| **Kidneys** | 0.26 |
| **Heart contents** | 9.17 |
| **Heart wall** | 0.26 |
| **Muscle** | 5.94 |
| **Lungs** | 0.20 |
| **Spleen** | 0.33 |
| **Liver** | 15.90 |
| **Red marrow** | 0.99 |
| **Cort bone** | 3.90 |
| **Remainder** | 7.33 |

dependency to the size of nano-particles, because the size larger than 10$\mu$m of nano-particles results in the accumulation in the lung, while the nano-particles over 100 nm (0.2 – 3 $\mu$m) cumulate favourably in the spleen and liver, and the nano-particles less than 30 nm are located in the bone marrow (9, 36-38).

Comparing the result of the intratumoral injection obtained in this study with those from the studies investigating the labelling PAMAM by other radionuclides such as $^{177}$Lu (39) and $^{188}$Re (40) revealed that the retention time for $^{177}$Lu-PAMAM, $^{188}$Re-PAMAM, and $^{47}$Sc-PAMAM in tumors were almost similar, and more than 90% of the injected dose remained in the tumors. The absorbed dose by intratumoral injection of $^{177}$Lu-PAMAM was discovered to be 3.01 Gy/MBq (41). In this study, the residence time for mice-tumor (0.1 g weight, 0.5 cm diameter) was 4.35h, and the tumor absorbed dose was 3.69Gy/MBq by considering 0.236 mGy/MBq-s for the S-value.

Finally, the estimation of absorbed dose of scandium-47 in human organs was performed by using PAMAM-G5 dendrimer encapsulated radio-scandium and giving vein injection to vital organs. However, it was recommended that further preclinical investigations should be carried out in order to evaluate the biokinetics, dosimetry, and, toxicity of this radiopharmaceutical.

### 5.1. Conclusions

In sum, the nano-radiopharmaceutical of radio-scandium with PAMAM G5 showed high performance and

**Table 4.** The Estimated Human Absorbed Dose From $^{47}$Sc-PAMAM by MIRD Schema

| Target Organ | Total Dose | | Primary Contributor (%) | | Secondary Contributor (%) | |
|---|---|---|---|---|---|---|
| | mGy/MBq | rad/mCi | | | | |
| **Adrenals** | 5.56E-02 | 2.06E-01 | Rem. body | 39.20 | Liver | 38.00 |
| **Brain** | 2.45E-02 | 9.06E-02 | Rem. body | 91.00 | Cort bone | 5.70 |
| **Breasts** | 3.29E-02 | 1.22E-01 | Rem. body | 63.60 | Heart Conte | 20.80 |
| **Gallbladder wall** | 7.03E-02 | 2.60E-01 | Liver | 59.10 | Rem. body | 31.40 |
| **LLI wall** | 1.23E-01 | 4.54E-01 | LLI | 85.60 | Rem. body | 10.50 |
| **Small intestine** | 3.35E-02 | 1.24E-01 | Rem. body | 68.90 | Liver | 16.80 |
| **Stomach** | 6.05E-02 | 2.24E-01 | Stomach | 53.90 | Rem. body | 20.00 |
| **ULI wall** | 3.63E-02 | 1.34E-01 | Rem. body | 63.00 | Liver | 24.90 |
| **Heart wall** | 1.11E+00 | 4.11E+00 | Heart content | 92.2 | Heart wall | 7.20 |
| **Kidneys** | 1.07E-01 | 3.98E-01 | Kidneys | 79.40 | Liver | 13.20 |
| **Liver** | 8.79E-01 | 3.25E+00 | Liver | 98.80 | Heart conte | 0.70 |
| **Lungs** | 4.72E-02 | 1.75E-01 | Lungs | 41.10 | Heart conte | 26.90 |
| **Muscle** | 3.17E-02 | 1.17E-01 | Muscle | 68.80 | Liver | 11.50 |
| **Ovaries** | 3.01E-02 | 1.11E-01 | Rem. body | 75.70 | Muscle | 8.50 |
| **Pancreas** | 5.42E-02 | 2.01E-01 | Rem. body | 40.80 | Liver | 34.30 |
| **Red marrow** | 6.66E-02 | 2.47E-01 | Red marrow | 64.40 | Rem. Body | 17.70 |
| **Bone surfaces** | 1.55E-01 | 5.73E-01 | Cort bone | 80.30 | Red marrow | 15.30 |
| **Skin** | 2.52E-02 | 9.31E-02 | Rem. body | 81.40 | Liver | 7.10 |
| **Spleen** | 1.91E-01 | 7.06E-01 | Spleen | 93.20 | Liver | 1.90 |
| **Testes** | 2.42E-02 | 8.96E-02 | Rem. body | 89.10 | Muscle | 7.40 |
| **Thymus** | 5.24E-02 | 1.94E-01 | Heart content | 46.8 | Rem. body | 40.90 |
| **Thyroid** | 2.70E-02 | 1.00E-01 | Rem. body | 80.70 | Muscle | 7.70 |
| **Urin bladder wall** | 2.70E-02 | 9.99E-02 | Rem. body | 83.50 | Muscle | 9.30 |
| **Uterus** | 2.91E-02 | 1.08E-01 | Rem. body | 79.30 | Muscle | 8.80 |
| **Total body** | 6.43E-02 | 2.38E-01 | Liver | 40.70 | Rem. body | 18.40 |
| **Effective dose equivalent** | 1.76E-01 (mSv/MBq) | 6.52E-01 (rem/mCi) | Remainder | 82.10 | Red marrow | 4.50 |
| **Effective dose** | 1.01E-01 (mSv/MBq) | 3.72E-01 (rem/mCi) | Liver | 43.70 | Colon | 14.60 |

acceptable radiochemical purity (~ 99%) as well as in vivo stability. Direct injection to the tumor was found to cause negligible leakage to other tissues, and the adequacy of radio-nano-complex in diminishing the size of the tumor was detected to be up to 39.24%. Radiochemical evaluation revealed that the radio-nano-compound may have been synthesized in a high yield of PAMAM-G5 dendrimer encapsulated radio-scandium.

The preclinical findings from our study indicated that $^{47}$Sc-PAMAM-G5 dendrimer encapsulated radio-scandium may have produced favorable results in small animal models. owever, it was recommended that further clinical studies should be conducted on larger animals before generalizing these results to human patients and developing therapeutic radiopharmaceutical for future solid tumors therapy.

## Footnotes

**Authors' Contribution:** Study concept and design: L.M. and S.S.; acquisition of data: N.A. and F.J.; analysis and interpretation of data: L.M.; drafting of the manuscript: L.M. and N.A.; critical revision of the manuscript for important

intellectual content: L.M. and S.S.; statistical analysis: M.A.; study supervision: L.M.

**Conflict of Interests:** There is no conflict of interest.

**Data Reproducibility:** The dataset presented in the study is available on request from the corresponding author during submission or after its publication.

**Ethical Approval:** This study has been performed under super vision of Nuclear Sciences and Technology Research Institute (NSTRI).

**Funding/Support:** The funding was provided by Nuclear Sciences and Technology Research Institute (NSTRI).

## References


1. Ting G, Chang CH, Wang HE. Cancer nanotargeted radiopharmaceuticals for tumor imaging and therapy. *Anticancer Res*. 2009;**29**(10):4107–18. [PubMed: 19846958].
2. Ting G, Chang CH, Wang HE, Lee TW. Nanotargeted radionuclides for cancer nuclear imaging and internal radiotherapy. *J Biomed Biotechnol*. 2010;**2010**. doi: 10.1155/2010/953537. [PubMed: 20811605]. [PubMed Central: PMC2929518].
3. Dancey G, Begent RH, Meyer T. Imaging in targeted delivery of therapy to cancer. *Target Oncol*. 2009;**4**(3):201–17. doi: 10.1007/s11523-009-0119-8. [PubMed: 19838639].
4. Eriksson D, Stigbrand T. Radiation-induced cell death mechanisms. *Tumour Biol*. 2010;**31**(4):363–72. doi: 10.1007/s13277-010-0042-8. [PubMed: 20490962].
5. Fritzberg AR, Berninger RW, Hadley SW, Wester DW. Approaches to radiolabeling of antibodies for diagnosis and therapy of cancer. *Pharm Res*. 1988;**5**(6):325–34. doi: 10.1023/a:1015995208444. [PubMed: 3072555].
6. Goerner M, Seiwert TY, Sudhoff H. Molecular targeted therapies in head and neck cancer–an update of recent developments. *Head Neck Oncol*. 2010;**2**:8. doi: 10.1186/1758-3284-2-8. [PubMed: 20398256]. [PubMed Central: PMC2868849].
7. Harrison J, Day P. Radiation doses and risks from internal emitters. *J Radiol Prot*. 2008;**28**(2):137–59. doi: 10.1088/0952-4746/28/2/R01. [PubMed: 18495991].
8. Ugur O, Kostakoglu L, Hui ET, Fisher DR, Garmestani K, Gansow OA, et al. Comparison of the targeting characteristics of various radioimmunoconjugates for radioimmunotherapy of neuroblastoma: dosimetry calculations incorporating cross-organ beta doses. *Nucl Med Biol*. 1996;**23**(1):1–8. doi: 10.1016/0969-8051(95)02001-2. [PubMed: 9004907].
9. Mohanraj VJ, Chen Y. Nanoparticles - A review. *Trop J Pharm Res*. 2007;**5**(1). doi: 10.4314/tjpr.v5i1.14634.
10. Patri AK, Majoros IJ, Baker JR. Dendritic polymer macromolecular carriers for drug delivery. *Curr Opin Chem Biol*. 2002;**6**(4):466–71. doi: 10.1016/s1367-5931(02)00347-2. [PubMed: 12133722].
11. Majoros IJ, Thomas TP, Mehta CB, Baker JJ. Poly(amidoamine) dendrimer-based multifunctional engineered nanodevice for cancer therapy. *J Med Chem*. 2005;**48**(19):5892–9. doi: 10.1021/jm0401863. [PubMed: 16161993].
12. Shultz MD, Duchamp JC, Wilson JD, Shu CY, Ge J, Zhang J, et al. Encapsulation of a radiolabeled cluster inside a fullerene cage, (177)Lu(x)Lu((3-x))N@C(80): an interleukin-13-conjugated radiolabeled metallofullerene platform. *J Am Chem Soc*. 2010;**132**(14):4980–1. doi: 10.1021/ja9093617. [PubMed: 20307100]. [PubMed Central: PMC2875150].
13. Stiriba SE, Frey H, Haag R. Dendritic polymers in biomedical applications: from potential to clinical use in diagnostics and therapy. *Angew Chem Int Ed Engl*. 2002;**41**(8):1329–34. doi: 10.1002/1521-3773(20020415)41:8<1329::aid-anie1329>3.0.co;2-p. [PubMed: 19750755].
14. Tomalia DA, Naylor AM, Goddard WA. Starburst Dendrimers: Molecular-Level Control of Size, Shape, Surface Chemistry, Topology, and Flexibility from Atoms to Macroscopic Matter. *Angewandte Chemie International Edition in English*. 1990;**29**(2):138–75. doi: 10.1002/anie.199001381.
15. Zhao M, Crooks RM. Intradendrimer Exchange of Metal Nanoparticles. *Chem Mater*. 1999;**11**(11):3379–85. doi: 10.1021/cm990435p.
16. Esfand R, Tomalia DA. Poly(amidoamine) (PAMAM) dendrimers: from biomimicry to drug delivery and biomedical applications. *Drug Discov Today*. 2001;**6**(8):427–36. doi: 10.1016/s1359-6446(01)01757-3.
17. Majoros I, Thomas T, Baker J. *Molecular engineering in nanotechnology: engineered drug delivery*. Valencia, CA, USA: American Scientific Publishers; 2006.
18. Saluja V, Mishra Y, Mishra V, Giri N, Nayak P. Dendrimers based cancer nanotheranostics: An overview. *Int J Pharm*. 2021;**600**:120485. doi: 10.1016/j.ijpharm.2021.120485. [PubMed: 33744447].
19. Sarko D, Eisenhut M, Haberkorn U, Mier W. Bifunctional chelators in the design and application of radiopharmaceuticals for oncological diseases. *Curr Med Chem*. 2012;**19**(17):2667–88. doi: 10.2174/092986712800609751. [PubMed: 22455579].
20. Muller C, Bunka M, Haller S, Koster U, Groehn V, Bernhardt P, et al. Promising prospects for 44Sc-/47Sc-based theragnostics: application of 47Sc for radionuclide tumor therapy in mice. *J Nucl Med*. 2014;**55**(10):1658–64. doi: 10.2967/jnumed.114.141614. [PubMed: 25034091].
21. Lenarczyk M, Goddu SM, Rao DV, Howell RW. Biologic dosimetry of bone marrow: induction of micronuclei in reticulocytes after exposure to 32P and 90Y. *J Nucl Med*. 2001;**42**(1):162–9. [PubMed: 11197968].
22. Aghaei-Amirkhizi N, Moghaddam-Banaem L, Athari-Allaf M, Sadjadi S, Johari-Daha F. Development of Dendrimer Encapsulated Radio-Ytterbium and Biodistributionin Tumor Bearing Mice. *IEEE Trans Nanobiosci*. 2016;**15**(6):549–54. doi: 10.1109/TNB.2016.2587906. [PubMed: 27824577].
23. Aghaei-Amirkhizi N. Preparation and Characterization of Dendrimer-Encapsulated Ytterbium Nanoparticles to produce a New Nano-Radio Pharmaceutical. *J Label Compd Radiopharm*. 2015.
24. Deilami-Nezhad L, Moghaddam-Banaem L, Sadeghi M. Development of bone seeker radiopharmaceuticals by Scandium-47 and estimation of human absorbed dose. *Appl Radiat Isot*. 2017;**129**:108–16. doi: 10.1016/j.apradiso.2017.07.062. [PubMed: 28843158].
25. Deilami-Nezhad L, Moghaddam-Banaem L, Sadeghi M, Asgari M. Production and purification of Scandium-47: A potential radioisotope for cancer theranostics. *Appl Radiat Isot*. 2016;**118**:124–30. doi: 10.1016/j.apradiso.2016.09.004. [PubMed: 27640172].
26. Moghaddam-Banaem L, Jalilian AR, Pourjavid M, Radfar E, Bahrami-Samani A, Yavari K, et al. Development of a radioscandium immunoconjugate for radioimmunotherapy. *Radiochimica Acta*. 2012;**100**(3):215–21. doi: 10.1524/ract.2012.1902.
27. Baer RW, Payne BD, Verrier ED, Vlahakes GJ, Molodowitch D, Uhlig PN, et al. Increased number of myocardial blood flow measurements with radionuclide-labeled microspheres. *Am J Physiol*. 1984;**246**(3 Pt 2):H418–34. doi: 10.1152/ajpheart.1984.246.3.H418. [PubMed: 6703077].

28. Wehner AP, Wilerson CL, Stevens DL. Lung clearance of neutron-activated Mount St. Helens volcanic ash in the rat. *Environ Res*. 1984;**35**(1):211–7. doi: 10.1016/0013-9351(84)90129-4.
29. Mutsuo I, Kazuhisa K. Cosmogenic radionuclides in meteorites including recently fallen ones-Constraints on the exposure history of chondrites. *Chikyukagaku (Geochcmistry)*. 2001;**35**:13–25.
30. Islam T, Harisinghani MG. Overview of nanoparticle use in cancer imaging. *Cancer Biomark*. 2009;**5**(2):61–7. doi: 10.3233/CBM-2009-0578. [PubMed: 19414922].
31. Eichman JD, Bielinska AU, Kukowska-Latallo JF, Baker JR. The use of PAMAM dendrimers in the efficient transfer of genetic material into cells. *Pharm Sci Technol Today*. 2000;**3**(7):232–45. doi: 10.1016/s1461-5347(00)00273-x.
32. Fathi F, Moghaddam-Banaem L, Shamsaei M, Samani A, Maragheh MG. Production, biodistribution, and dosimetry of (47)Sc-1,4,7,10-tetraazacyclododecane-1,4,7,10-tetramethylene phosphonic acid as a bone-seeking radiopharmaceutical. *J Med Phys*. 2015;**40**(3):156–64. doi: 10.4103/0971-6203.165078. [PubMed: 26500402]. [PubMed Central: PMC4594385].
33. Stabin MG. *Fundamentals of nuclear medicine dosimetry*. Springer Science & Business Media; 2008.
34. Valentin J. Basic anatomical and physiological data for use in radiological protection: reference values. *Ann ICRP*. 2016;**32**(3-4):1–277. doi: 10.1016/s0146-6453(03)00002-2.
35. Siegel JA, Thomas SR, Stubbs JB, Stabin MG, Hays MT, Koral KF, et al. MIRD pamphlet no. 16: Techniques for quantitative radiopharmaceutical biodistribution data acquisition and analysis for use in human radiation dose estimates. *J Nucl Med*. 1999;**40**(2):37S–61S. [PubMed: 10025848].
36. Blanco E, Shen H, Ferrari M. Principles of nanoparticle design for overcoming biological barriers to drug delivery. *Nat Biotechnol*. 2015;**33**(9):941–51. doi: 10.1038/nbt.3330. [PubMed: 26348965]. [PubMed Central: PMC4978509].
37. He C, Hu Y, Yin L, Tang C, Yin C. Effects of particle size and surface charge on cellular uptake and biodistribution of polymeric nanoparticles. *Biomaterials*. 2010;**31**(13):3657–66. doi: 10.1016/j.biomaterials.2010.01.065. [PubMed: 20138662].
38. Kulkarni SA, Feng SS. Effects of particle size and surface modification on cellular uptake and biodistribution of polymeric nanoparticles for drug delivery. *Pharm Res*. 2013;**30**(10):2512–22. doi: 10.1007/s11095-012-0958-3. [PubMed: 23314933].
39. Mendoza-Nava H, Ferro-Flores G, Ramírez FDM, Ocampo-García B, Santos-Cuevas C, Aranda-Lara L, et al. 177Lu-Dendrimer Conjugated to Folate and Bombesin with Gold Nanoparticles in the Dendritic Cavity: A Potential Theranostic Radiopharmaceutical. *J Nanomater*. 2016;**2016**:1–11. doi: 10.1155/2016/1039258.
40. Cui W, Zhang Y, Xu X, Shen YM. Synthesis and 188Re radiolabelling of dendrimer polyamide amine (PAMAM) folic acid conjugate. *Med Chem*. 2012;**8**(4):727–31. doi: 10.2174/157340612801216256. [PubMed: 22548334].
41. Gibbens-Bandala B, Morales-Avila E, Ferro-Flores G, Santos-Cuevas C, Luna-Gutierrez M, Ramirez-Nava G, et al. Synthesis and Evaluation of (177)Lu-DOTA-DN(PTX)-BN for Selective and Concomitant Radio and Drug-Therapeutic Effect on Breast Cancer Cells. *Polymers (Basel)*. 2019;**11**(10). doi: 10.3390/polym11101572. [PubMed: 31569625]. [PubMed Central: PMC6835492].